Determination of the spin density distribution in the organic conductor DMTM(TCNQ)2 with 13C magic angle spinning NMR

Kolbert, A.C.; Verel, R.; Groot, H.J.M. de; Almeida, M.

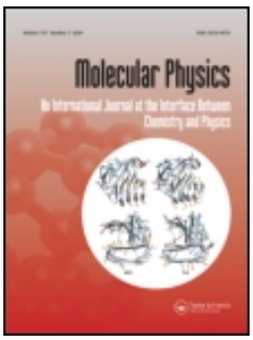

Molecular Physics

ISSN: 0026-8976 (Print) 1362-3028 (Online) Journal homepage: https://www.tandfonline.com/loi/tmph20

Determination of the spin density distribution in the organic conductor DMTM(TCNQ)2 with 13C magic angle spinning NMR

ANDREW C. KOLBERT , RENE VEREL , HUUB DE GROOT & MANUEL ALMEIDA

To cite this article: ANDREW C. KOLBERT , RENE VEREL , HUUB DE GROOT & MANUEL ALMEIDA (1997) Determination of the spin density distribution in the organic conductor DMTM(TCNQ)2 with 13C magic angle spinning NMR, Molecular Physics, 91:4, 725-730, DOI: 10.1080/002689797171210

To link to this article: https://doi.org/10.1080/002689797171210

Published online: 03 Dec 2010.

MOLECULAR PHYSICS, 1997, VOL. 91, NO. 4, 725–730

Determination of the spin density distribution in the organic conductor DMTM(TCNQ)$_2$ with ^{13}C magic angle spinning NMR

By ANDREW C. KOLBERT†, RENE VEREL‡, HUUB DE GROOT and MANUEL ALMEIDA§

Gorlaeus Laboratoria, Rijks Universiteit te Leiden, NL-2300 RA Leiden, The Netherlands

§ Dept. Quimica, National Laboratory for Engineering and Industrial Technology, 2686 Sacavem Codex, Portugal

(*Received 29 July 1996; revised version accepted 18 February 1997*)

^{13}C magic angle spinning (MAS) NMR experiments on the organic conductor *N*,*N*-dimethyl-thiomorpholinium bis-tetracyanoquino-dimethane [DMTM(TCNQ)$_2$] isotopically enriched at the position of the C-2 carbons of TCNQ are reported. Two isotropic resonances are resolved above the structural phase transition at 272 K, both exhibiting large positive isotropic and anisotropic Knight shifts. Sideband analysis of the MAS spectra has yielded the complete Knight shift tensors above T_c, in the insulating state. From the Knight shifts the hyperfine couplings and spin densities at the C-2 sites were calculated and were found to be in good agreement with molecular calculations. Below T_c, the sideband pattern displays two sets of ^{13}C-2 lines indicating a spin density distribution between two sites of 0·59 : 0·41.

1. Introduction

The organic conductor *N*,*N*-dimethyl-thiomorpholinium bis-tetracyanoquino-dimethane [DMTM(TCNQ)$_2$] has been the focus of a great deal of attention of late, due to its unusual first order phase transition at T_c = 272 K [1–9]. Upon *cooling* through 272 K DMTM(TCNQ)$_2$ changes from an E_g = 0·25 eV gap semiconductor to a state with an almost temperature independent conductivity, nearly three orders of magnitude higher.

The complete crystal structure has been determined by *X*-ray diffraction, above the phase transition. The unit cell is monoclinic with space group $P2_1/m$, and the DMTM cation is located on a mirror plane between two equivalent sheets of parallel, dimerized TCNQ stacks [5]. The dimerized TCNQ molecules within a stack are related by inversion centres. Below T_c, the unit cell changes to triclinic, the mirror plane is gone, probably due to the ordering of the DMTMs, and the two parallel TCNQ stacks become inequivalent.

Recently, high resolution solid state NMR has been applied to gain insight into the details of the electronic phase transition via measurement of the ^{13}C and ^{1}H Knight shifts [7–9]. Solid state NMR is an indispensable tool in these studies as it is the only way of obtaining a measurement of the magnetic susceptibility, i.e. the local spin density, with atomic site resolution [10]. Magic angle spinning (MAS) [7] and single crystal ^{13}C [9] studies of the C-1 (cyano) site, below T_c, have identified lines corresponding to sites on different stacks with substantially different spin densities. The combination of multiple pulse and MAS has been applied to obtain high resolution ^{1}H spectra above and below T_c, which also exhibit lines corresponding to sites with very different spin densities [8]. In this case, however, the assignment of the lines to different stacks was ambiguous.

These results supported a model proposed to explain the conductivity anomaly, involving an interstack charge transfer at T_c [2]. The interstack charge transfer, presumably aided by the directed dipole moment of the ordered cations below T_c, allows the conduction bands of both stacks to become partially filled, thus explaining the rise in conductivity at T_c. Unfortunately all of the NMR measurements to date have focused on sites with very low spin densities. Extrapolating the measurement of spin densities at sites with only a few percent of the total spin density, to the movement of a substantial amount of electron density through the phase transition, is arguably questionable.

In this paper we report ^{13}C MAS NMR measurements of the Knight shifts at the site where the spin density is the largest–the C-2 carbons (see figure 1) on which the p_z orbitals reside whose overlap contributes to

† Present address: DSM Copolymer Inc., PO Box 2591, Baton Rouge, Louisiana 70821, USA.

‡ Present address: Department of Physical Chemistry; Katholieke Universiteit Nijmegen; Toernooiveld 1, The Netherlands.

0026–8976/97 $12·00

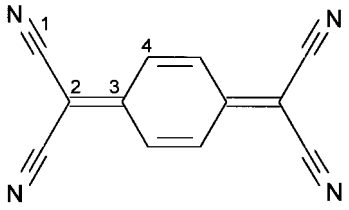

Figure 1. Tetracyanoquino-dimethane (TCNQ) with site numbering as in text. The C-2 carbons are ^{13}C labelled.

the extended π system within a stack. MAS spectra have been acquired both above and below the phase transition. Above the phase transition, fits to the spectra have yielded the complete Knight shift tensors of all sites, from which the hyperfine coupling tensors and spin densities have been calculated. These results are shown to be in good agreement with the results of molecular calculations. Below the phase transition, two sets of lines are observed, and the ratio of the spin densities is calculated from the ratio of K_{33} of the respective Knight shift tensors. The differences in the distribution of spin densities above and below T_c are compared with previous NMR measurements at different atomic sites.

2. Magic angle spinning NMR of organic conductors

The resonances in the NMR spectrum are always shifted relative to the Larmor frequency. In diamagnetic solids this shift is due to the shielding of the magnetic field by the electrons, and is called a chemical shift as it is indicative of the chemical identity of the fragment involved, and is largely transferable between molecules. In organic conductors there is an additional shift due to the averaged hyperfine interaction to the conduction electrons, which is called the Knight shift [11]. The Knight shift is related to the hyperfine interaction through

$$\mathbf{K} = \frac{\chi_s}{\hbar\gamma_e\gamma_n}\mathbf{A} \qquad (1)$$

in which χ_s is the spin susceptibility per conduction electron, γ_e and γ_n are the electron and nuclear gyromagnetic ratios, and **A** is the hyperfine tensor which encompasses all interactions of the nuclei with the conduction electrons including the Fermi contact term, dipolar interactions and core–polarization effects.

In the case of metals, this shift is due to uncorrelated electrons moving at the Fermi velocity. The case of organic conductors is somewhat more complex. The electronic properties of the singly occupied molecular orbitals can be described with the Hubbard Hamiltonian:

$$H = H_{tb} + H_{os} \qquad (2)$$

consisting of a tight-binding term:

$$H_{tb} = -t\sum_j \left(c^+_{(j,\sigma)}c_{(j+1,\sigma)} + c^+_{(j+1,\sigma)}c_{(j,\sigma)}\right) \qquad (3)$$

and a term describing the on-site interaction:

$$H_{os} = U\sum_j \left(n_{(j,\sigma)}n_{(j,-\sigma)}\right) \qquad (4a)$$

with the number operator

$$n_{(j,\sigma)} = c^+_{(j,\sigma)}c_{(j,\sigma)} \qquad (4b)$$

in which U is the on-site energy, t is the transfer integral, j is the site index, σ is the spin index, and c and c^+ are the electron annihilation and creation operators, respectively. For $DMTM(TCNQ)_2$ at room temperature, $U \cong 1{\cdot}4$ eV and $t < 0{\cdot}2$ eV, therefore $U \gg t$ and the system becomes a Mott–Hubbard insulator. In this situation each TCNQ dimer contains one localized electron spin, antiferromagnetically coupled to its neighbours on the stack, with spin correlations propagating rapidly along each stack. The Hubbard Hamiltonian then simplifies into:

$$H = -2J\sum_j S_jS_{j+1} \qquad (5)$$

with

$$J = -\frac{t^2}{U}$$

for the description of an antiferromagnetic Heisenberg (isotropic) spin chain. For $DMTM(TCNQ)_2$, $J/k_B = -50$ K, from the temperature of the decrease in the magnetic susceptibility [1], leading to an estimate of the correlation time $\tau_c = 10^{-12}$ s. As this is rapid in comparison to the NMR time scale ($\approx 10^{-8}$ s), a net electron spin interaction results after averaging of the hyperfine interactions via the antiferromagnetic fluctuations present within a stack. Such antiferromagnetic fluctuations are thus crucial to the mechanism for the Knight shifts observed in several semiconductors [12].

As the Knight shift is a second rank tensor with a large anisotropic contribution, MAS can be employed in order to obtain single site resolution in a polycrystalline sample [13, 14]. MAS, in the regime in which the spinning speed is slow compared with the breadth of the anisotropy, converts the static powder lineshape into a manifold of rotational sidebands spaced at integral multiples of the spinning speed, with the centre of gravity at the isotropic shift frequency [15]. The complete tensor may be recovered from such a spectrum by a fit to the sideband intensities [16].

For the case of organic conductors, the problem does not end there as, in general, the total shift observed in the NMR spectum of an organic conductor will be the

sum of the chemical and Knight shift tensors and is given by [9, 10]

$$\delta = \sigma + \mathbf{K} \qquad (6)$$

which also defines the relative sign conventions for the chemical and Knight shifts. Fits to the magic angle spinning spectra will yield the sum tensor δ. The Knight shift tensors must then be extracted by subtracting the chemical shift tensor σ from δ. The chemical shift tensor of the site in the organic conductor may not be determined independently, but as σ is largely a transferable quantity, the use of a neutral reference compound for σ, such as TCNQ for TNCQ salts, has been established as a reliable method for separating the interactions [17]. The relative orientation of σ and δ necessary for the subtraction are, in general, unknown; however, they can be reasoned by means of geometric arguments as will be shown below. Once **K** has been determined, the hyperfine coupling tensor may be easily calculated.

3. Results

Figure 2(*a*) shows the ^{13}C MAS spectrum of ^{13}C-2 labelled DMTM(TCNQ)$_2$, spinning at $\omega_r/2\pi$ = 18·000 kHz, above T_c. Two sideband patterns are clearly resolved, both with large positive isotropic and anisotropic shifts. The isotropic resonances were identified by acquiring spectra at different spinning speeds and are marked with asterisks. A least squares fit of the simulations of MAS tensors by Herzfeld and Berger [16] to the spectrum has yielded the total shift tensor values of δ. A simulation using the parameters from the best fit is shown in figure 2(*b*). The agreement is quite good, though there are deviations to the high frequency side of the spectrum which are probably due to the limited probe response.

In order to obtain the Knight shift tensor **K** from δ, we must subtract the contribution from σ, the chemical shift tensor. The principal values of the chemical shift tensor of ^{13}C-2 enriched TCNQ, determined via Herzfeld–Berger sideband analysis of MAS spectra, are σ_{11} = 40 ppm, σ_{22} = 75 ppm, σ_{33} = 157 ppm [17]. In order to orient the chemical shift tensor in its principal axis system for the C-2 site of TCNQ, we should compare it with a chemical shift tensor of the same symmetry, for which the full CSA tensor in its principal axis system has been determined. The traceless CSA tensor of ethylene has been both calculated theoretically, σ_{11} = - 149 ppm, σ_{22} = 29 ppm, σ_{33} = + 120 ppm [18], and measured experimentally [19], σ_{11} = - 103 ppm, σ_{22} = - 3 ppm, σ_{33} = + 106 ppm. These results place the intermediate tensor value along the double bond with the least shielded value, σ_{33}, out of the plane of the molecule. In correspondence with ethylene we can orient the traceless tensor for TCNQ σ_{11} = - 50·7 ppm, σ_{22} = - 15·7 ppm, σ_{33} = 66·4 ppm so that σ_{33} is out of the plane of the TCNQ molecule. The choice of the axes of the other two tensor values should be made such that **K** is most nearly axially symmetric. Thus we obtain the principal values of **K**

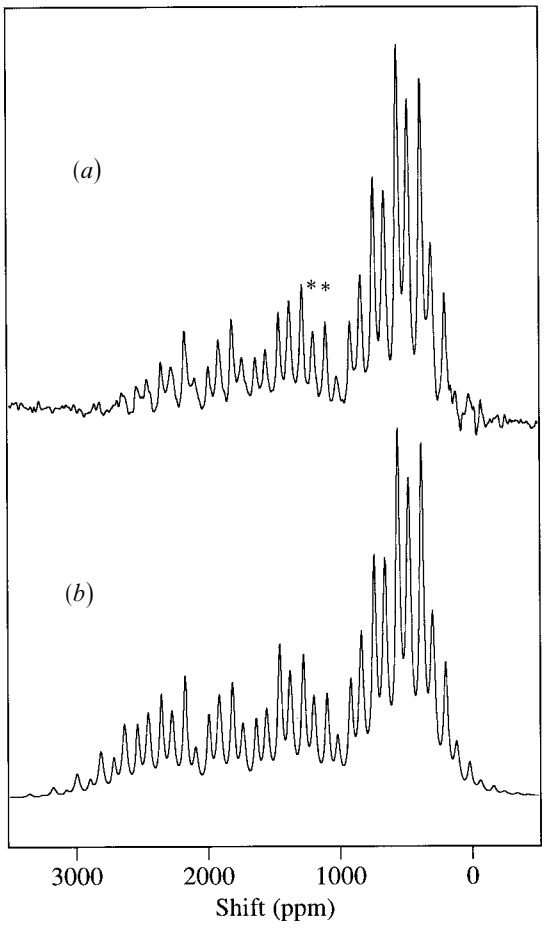

Figure 2. (*a*) MAS NMR Spectrum of ^{13}C-2 DMTM(TCNQ)$_2$ at 300 K. The isotropic shifts are illustrated with asterisks and are referenced to TMS. The spinning speed was $\omega_r/2\pi$ = 18·000 kHz, 50 000 scans were added with a recycle time of 30 ms. (*b*) A simulation using parameters derived from the best fit to the derivative of the spectrum in (*a*); $\delta_{iso,I}$ = 1094 ppm, $\delta_{11,I}$ = 244 ppm, $\delta_{22,I}$ = 269 ppm, $\delta_{33,I}$ = 2770 ppm, $\delta_{iso,II}$ = 1193 ppm, $\delta_{11,II}$ = 274 ppm, $\delta_{22,II}$ = 275 ppm, $\delta_{33,II}$ = 3031 ppm.

$$\begin{aligned} K_{11} &= \delta_{11} - \sigma_{11} \\ K_{22} &= \delta_{22} - \sigma_{22} \\ K_{33} &= \delta_{33} - \sigma_{33} \end{aligned} \qquad (7)$$

which are listed in table 1 along with the hyperfine coupling constants calculated from equation (1) using χ_s from [1].

Below T_c, at 250 K, we obtain the spectrum of figure 3 with $\omega_r/2\pi$ = 12·5 kHz. One can see two resolved sideband patterns, one relatively intense set of lines

Table 1. Isotropic and anisotropic Knight shift tensor values, above T_c, obtained from best fit to the spectrum of figure 2, after correcting for the presence of the chemical shift. Isotropic positions are accurate to ±2 ppm and principal values of tensors are accurate to ±15 ppm.

Site	K_{iso} (ppm)	K_{11} (ppm)	K_{22} (ppm)	K_{33} (ppm)	a_{iso} (MHz)	a_{11} (MHz)	a_{22} (MHz)	a_{33} (MHz)
I	1003	204	194	2613	11·3	2·3	2·2	29·4
II	1103	234	200	2874	12·4	2·6	2·3	32·2

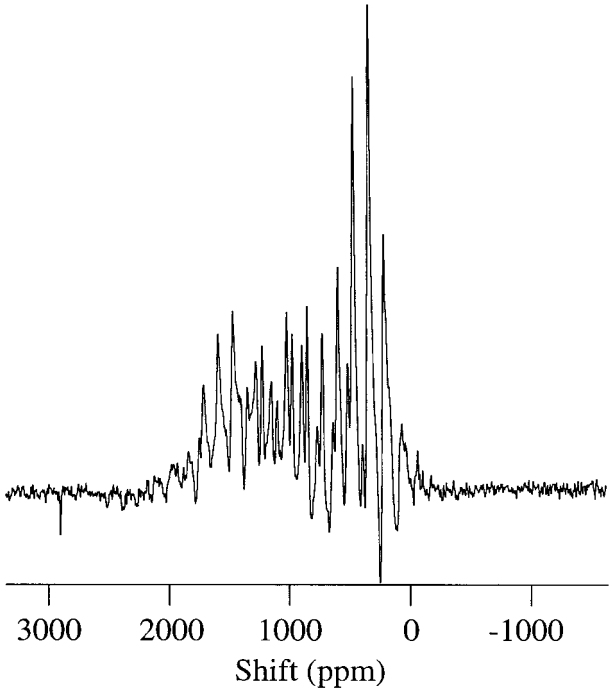

Figure 3. ^{13}C MAS spectra of DMTM(TCNQ)$_2$ at T = 250 K, $\omega_r/2\pi$ = 12·5 kHz, 700 000 scans were added with a recycle time of 30 ms. Slight phase errors to the high frequency side of the spectrum are due to a small (~ 0·1 μs) synchronization error of the π-pulse with respect to the rotational echo.

extending from 0–1800 ppm and a broader, less intense manifold of sidebands extending to approximately 2500 ppm. The quality of the spectrum makes any but a qualitative analysis impossible, however, from the ratio of the estimated δ_{33} values (2500 and 1800 ppm), we can calculate a spin density ratio ~ $K_{33,I} : K_{33,II}$ of 0·59 : 0·41, in line with previous ^{13}C and ^{1}H NMR measurements on different atomic sites [7–9].

4. A comparison with molecular calculations for the TCNQ anion

A comparison of the hyperfine tensors measured with the results of molecular calculations requires a method for calculating **A** given the distribution of spin densities. The traceless, and therefore purely dipolar, part of the hyperfine coupling tensor can be written as

$$\mathbf{A} = \mathbf{A}(\text{local}) + \sum_n \mathbf{A}_n \tag{8}$$

in which **A** (local) is the on-site term resulting from the unpaired π-spin density centred on the carbon atom of interest and $\sum_n \mathbf{A}_n$ represents the contribution due to π-spin densities residing on neighbouring carbon atoms. Though in principle, this sum runs over all atomic sites, the strong r^{-3} distance dependence of the dipolar interaction allows us to consider only nearest neighbour contributions. The on-site contribution to the hyperfine coupling tensor can be calculated by integrating the $2p_z$ hydrogenic wavefunction over all space obtaining

$$\mathbf{A}(\text{local}) = \frac{\mu_0}{5\pi}\gamma_e\gamma_n\hbar\left\langle\frac{1}{r_e^3}\right\rangle\begin{pmatrix} -1/2 & 0 & 0 \\ 0 & -1/2 & 0 \\ 0 & 0 & 1 \end{pmatrix}\rho_{\pi 2} \tag{9}$$

in which $\langle 1/r_e^3\rangle$ is the expectation value of $1/r_e^3$ over the p_z orbital and for a carbon atom is 11·49 A^{-3} [20–22]. The offsite contribution to **A** can be estimated by calculating the dipolar couplings to a point dipole $\gamma_e\hbar S$ centred at the site of the relevant nuclei and is given by

$$A_n(p,q) = \frac{-\gamma_c|\gamma_e|\hbar\rho_{\pi n}}{|\mathbf{r}_{cn}|^3}\left(\delta_{pq} - \frac{3x_p x_q}{|\mathbf{r}_{cn}|^2}\right) \tag{10}$$

in which x_p and x_q are the p and q components of **r** [22, 23]. For the case of the C-2 site in TCNQ, these equations can be written as

$$\begin{aligned}
A_{xx} &= \frac{\mu_0}{4\pi}\hbar\gamma_e\gamma_c\left(-\frac{2}{5}\left\langle\frac{1}{r_e^3}\right\rangle\rho_{\pi 2} + \frac{2}{r_{23}^3}\rho_{\pi 3} - \frac{1}{2r_{21}^3}\rho_{\pi 1}\right) \\
A_{yy} &= \frac{\mu_0}{4\pi}\hbar\gamma_e\gamma_c\left(-\frac{2}{5}\left\langle\frac{1}{r_e^3}\right\rangle\rho_{\pi 2} - \frac{1}{r_{23}^3}\rho_{\pi 3} + \frac{5}{2r_{21}^3}\rho_{\pi 1}\right) \\
A_{zz} &= \frac{\mu_0}{4\pi}\hbar\gamma_e\gamma_c\left(+\frac{4}{5}\left\langle\frac{1}{r_e^3}\right\rangle\rho_{\pi 2} - \frac{1}{r_{23}^3}\rho_{\pi 3} - \frac{2}{r_{21}^3}\rho_{\pi 1}\right)
\end{aligned} \tag{11}$$

in which $\rho_{\pi 1}$, $\rho_{\pi 2}$ and $\rho_{\pi 3}$ are the spin densities on the C-1, C-2, and C-3 carbons, respectively. r_{12} = 1·43 A and r_{23} = 1·39 A from the X-ray structure [5]. The spin densities from different molecular calculations and

Table 2. Experimental and calculated spin densities and hyperfine coupling constants.

Spin densities and couplings	Experimental site 1 (2)	Hückel [24]	UHF [25]	McLachlen [24]	INDO [26]
$\rho_{\pi 1}$	—	0·013	- 0·021	- 0·0005	- 0·048
$\rho_{\pi 2}$	0·197 (0·217)	0·225	0·241	0·297	0·303
$\rho_{\pi 3}$	—	0·050	0·028	0·010	- 0·022
A_{xx}(MHz)	- 9·0 (- 9·8)	- 9·9	- 10·8	- 13·5	- 13·9
A_{yy}(MHz)	- 9·1 (- 10·1)	- 10·3	- 11·3	- 13·7	- 14·2
A_{zz}(MHz)	18·1 (19·9)	20·3	22·1	27·1	28·1

their corresponding coupling tensors are presented in table 2 along with the experimental results above T_c. The spin densities of table 2 represent normalization of the spin density to unity over a TCNQ *molecule*, for the purpose of the comparison with molecular calculations. The spin density on the C-2 site has been calculated using equation (11) and the experimental values for A_{zz}. As the experimental results are influenced very little by off-site contributions, we have not calculated $\rho_{\pi 1}$ and $\rho_{\pi 3}$, but instead have used the Hückel results to calculate $\rho_{\pi 2}$ via equation (11). The correction to $\rho_{\pi 2}$ by using non-zero spin densities for $\rho_{\pi 1}$ and $\rho_{\pi 3}$ in equation (11), is less than 1%.

The experimental agreement with the Hückel [24] and unrestricted Hartree–Fock (UHF) [25] calculations is quite good. The INDO [26] and McLachlen [24] calculation methods give somewhat larger coupling constants than are observed experimentally, however the relative ratios of the components of **A** are still correct, the coupling constants differing by a scaling factor.

5. Experimental

99% ^{13}C-2 enriched TCNQ was synthesized from 1,4 cyclohexanedione and enriched malononitrile using a previously published procedure for unlabelled TCNQ [27]. The enriched malononitrile was synthesized using sodium cyanide and 99% bromoacetic-2-^{13}C acid [28]. The labelled DMTM(TCNQ)$_2$ was prepared via the reaction of the cation iodide with enriched TCNQ in boiling acetonitrile, as previously described [29, 30]. Magic angle spinning NMR experiments were performed on a Bruker MSL-400 spectrometer equipped with a 9·4 T superconducting magnet, and a 4 mm high speed, variable temperature MAS probe. Temperatures were maintained to within 2 K with a Bruker temperature controller, and spinning speeds were stabilized to within 5 Hz with a home-built spinning speed controller described elsewhere [31]. Spectra were acquired with a Hahn echo pulse sequence ($\pi/2$-τ-π-τ-acquire) with a $\pi/2$ pulse of 3·7 μs duration at the ^{13}C frequency. As the anisotropies were very large, precise rotor synchronization of the pulse sequence such that the π-pulse coincided with a rotational echo was critical to avoid phase distortions in the spectra. No ^{1}H decoupling was applied during acquisition as the rapid MAS (> 10 kHz) removed the weak ^{1}H-^{13}C dipolar couplings at the C-2 site. As spin-lattice relaxation times are on the order of 10 ms, recycle times of 30 ms were used allowing the rapid acquisition of many scans. Fits to the sideband manifolds were performed on a Silicon Graphics Indy workstation using the CERN 'Minuit' package incorporating the method of Herzfeld and Berger [15], previously described [13]. The spectra were fitted using the first derivative as this minimizes errors due to phasing problems in the wings of the spectrum.

6. Conclusions

The spin density distribution and the electronic changes at the structural phase transition in the organic conductor DMTM(TCNQ)$_2$ have been investigated with ^{13}C magic angle spinning NMR at the C-2 carbons, the sites of the greatest spin density. Two sites are resolved above T_c = 272 K, both exhibiting large positive Knight shifts, corresponding to a ratio of spin densities of 1·1 : 1. The calculated hyperfine couplings agree well with the results of molecular calculations. Below T_c, there are two sideband manifolds with a ratio of the spin densities between them of 0·59 : 0·41, in agreement with previous ^{1}H (0·65 : 0·35) [8] and ^{13}C NMR (0·62 : 0·38) [7,9] measurements below T_c on different sites.

We would like to thank Professor Michael Mehring and Ms Gisela Zimmer for helpful discussions, Dr J. M. Fabre for helpful suggestions concerning the synthesis of the labelled compounds, and Mr Cees Erkelens for experimental assistance.

References

[1] Oostra, S., De Boer, J. L., and De Lange, P., 1983, *J. Phys. (Paris) Colloq.*, **44,** C3-1387.
[2] Visser, R. J., Van Smaalen, S., De Boer, J. L., and Vos, A., 1985, *Molec. Cryst. Liq. Cryst.*, **120,** 167.
[3] Almeida, M., Alcacer, L., Oostra, S., and De Boer, J. L., 1987, *Synth. Method.*, **19,** 445.
[4] Rachdi, F., Ribet, M., Bernier, P., and Almeida, M., 1990, *Synth. Method*, **35,** 47.

[5] Visser, R. J., De Boer, J. L., and Vos, A., 1990, *Acta crystallogr.* C, **46,** 864.
[6] Zimmer, G., Kolbert, A. C., Rachdi, F., Bernier, P., Almeida, M., and Mehring, M., 1991, *Chem. Phys. Lett.*, **182,** 673.
[7] Rachdi, F., Nunes, T., Ribet, M., Bernier, P., Helmle, M., Mehring, M., and Almeida, M., 1992, *Phys. Rev.* B, **45,** 8134.
[8] Kolbert, A. C., Zimmer, G., Rachdi, F., Bernier, P., Almeida, M., and Mehring, M., 1992, *Phys. Rev.* B, **46,** 674.
[9] Zimmer, G., Kolbert, A. C., Mehring, M., Rachdi, F., Bernier, P., and Almeida, M., 1993, Phys. Rev. B, **47,** 763.
[10] Mehring, M., 1987, *Low Dimensional Conductors and Superconductors*, edited by D. Jerome and L. G. Caron (New York: Plenum).
[11] Knight, W., 1956, *Solid State Phys.*, **2,** 93.
[12] Kolbert, A. C., and Mehring, M., 1992, *J. magn. Reson.*, **100,** 82.
[13] Lowe, I. J., 1959, *Phys. Rev. Lett.*, **2,** 285.
[14] Andrew, E. R., Bradbury, A., and Eades, R. G., 1958, *Nature (Lond.)*, **182,** 1659.
[15] Maricq, M. M., and Waugh, J. S., 1979, *J. chem. Phys.*, **70,** 3300.
[16] Herzfield, J., and Berger, A., 1980, *J. chem. Phys.*, **73,** 6021.
[17] Nunes, T., Vainrub, A., Ribet, M., Rachdi, F., Bernier, P., and Almeida, M., 1992, *J. chem. Phys.*, **96,** 8021.
[18] Hansen, A. E., and Bouman, T. D., 1985 *J. chem. Phys.*, **82,** 5035.
[19] Zilm, K. W., and Grant, D. M., 1981, *J. Amer. Soc.*, **103,** 2913.
[20] Carrington, A., and McLachlen, A. D., 1969, *Introduction to Magnetic Resonance* (New York, Harper and Row).
[21] Symons, M., 1978, *Chemical and Biochemical Aspects of Electron Spin Resonance* (New York: Van Nostrand Reinhold).
[22] Klutz, T., Hennig, I., Haeberlen, U., and Schweitzer, D., *Appl. magn. Reson.* (in the press).
[23] Vainrub, A. M., Kheinmaa, I. A., and Yagubskii, E. B., 1987, *JETP Lett.*, **44,** 318.
[24] Rieger, P. H., Fraenkel, G. K., 1962, *J. Phys. (Paris)*, **37,** 2795.
[25] Lowitz, D. A., 1967, *J. chem. Phys.*, **46,** 4698.
[26] Werner, A., 1991, private communication.
[27] Acker, D. S., and Hertler, W. R., 1962, *J. Amer. chem. Soc.*, **84,** 3370.
[28] Vogel, A. I., 1964, *Practical Organic Chemistry*, 3rd Edn., (London: Longman Green), p. 433.
[29] Almeida, M., and Alcacer, L., 1983, *J. Cryst. Growth*, **62,** 183.
[30] Almeida, M., Alcacer, L., and Lindegaard-Andersen, A., 1985, *J. Cryst. Growth*, **72,** 567.
[31] de Groot, H. J. M., Smith, S. O., Kolbert, A. C., Courtin, J. M. L., Winkel, C., Lugtenburg, J., Herzfeld, J. and Griffin, R. G., 1991, *J. magn. Reson.*, **91,** 30.